# MAPK pathway activity plays a key role in PD-L1 expression of lung adenocarcinoma cells

Thijs S. Stutvoet[1]*, Arjan Kol[2]*, Elisabeth G.E. de Vries[1], Marco de Bruyn[2], Rudolf S.N. Fehrmann[1], Anton G.T. Terwisscha van Scheltinga[3], Steven de Jong[1+]

[1]Department of Medical Oncology, Cancer Research Center Groningen, University of Groningen, University Medical Center Groningen, Groningen, The Netherlands

[2]Department of Obstetrics and Gynecology, Cancer Research Center Groningen, University of Groningen, University Medical Center Groningen, Groningen, The Netherlands

[3]Department of Clinical Pharmacy and Pharmacology, University of Groningen, University Medical Center Groningen, Groningen, The Netherlands

* These authors contributed equally

[+]**Correspondence to:** Steven de Jong, PhD, Department of Medical Oncology, University Medical Center Groningen, Hanzeplein 1, 9713 GZ Groningen, The Netherlands. E-mail: s.de.jong@umcg.nl

**Running title:** MAPK signaling in growth factor- and cytokine-induced PD-L1 expression

**Conflict of interest statement:** The authors declare that they have no competing interests

**Word count for the main text: 3999**

**Abstract**

Immune checkpoint inhibitors targeting programmed cell death protein 1 (PD-1) and programmed death-ligand 1 (PD-L1) have improved the survival of patients with non-small cell lung cancer (NSCLC). Still, many patients do not respond to these inhibitors. PD-L1 (*CD274*) expression, one of the factors that influences efficacy of immune checkpoint inhibitors, is dynamic. Here, we studied the regulation of PD-L1 expression in NSCLC without targetable genetic alterations in EGFR, ALK, BRAF, ROS1, MET, ERBB2 and RET. Analysis of RNA sequencing data from these NSCLCs revealed that inferred IFNγ, EGFR and MAPK signaling correlated with *CD274* gene expression in lung adenocarcinoma. In a representative lung adenocarcinoma cell line panel, stimulation with EGF or IFNγ increased *CD274* mRNA and PD-L1 protein and membrane levels, which were further enhanced by combining EGF and IFNγ. Similarly, tumor cell PD-L1 membrane levels increased after coculture with activated PBMCs. Inhibition of the MAPK pathway, using EGFR inhibitors cetuximab and erlotinib or the MEK 1 and 2 inhibitor selumetinib, prevented EGF and IFNγ-induced *CD274* mRNA and PD-L1 protein and membrane upregulation, but had no effect on IFNγ-induced major histocompatibility complex 1 (MHC-I) upregulation. Interestingly, while IFNγ increases transcriptional activity of *CD274*, MAPK signaling also increased stabilization of *CD274* mRNA. In conclusion, MAPK pathway activity plays a key role in EGF- and IFNγ-induced PD-L1 expression in lung adenocarcinoma without targetable genetic alterations and may present a target to improve efficacy of immunotherapy.

**Key words:** non-small cell lung cancer (NSCLC), Programmed death-ligand 1 (PD-L1), interferon gamma (IFNγ), mitogen-activated protein kinase pathway (MAPK pathway), major histocompatibility complex class I (MHC-I).

**Introduction**

After years of limited progress in the treatment of advanced non-small cell lung cancer (NSCLC), a major leap forward has been made with the introduction of programmed cell death protein 1 (PD-1)/ programmed death-ligand 1 (PD-L1) targeting immune checkpoint inhibitors. These have greatly improved overall survival of patients with advanced NSCLC, especially in patients without targetable genetic alterations, accounting for almost 60% of NSCLC [1–3]. Patients with PD-L1 positive tumors generally respond better to PD-1 targeted immune checkpoint inhibition. However, discrepancies between observed PD-L1 expression and benefit from treatment often occur [4]; even in a preselected patient population with >50% PD-L1 positive tumor cells, only 45-55% of patients respond to therapy [5]. The limited value of tumor PD-L1 as a biomarker may be caused by the highly dynamic expression of PD-L1 due to the influence of multiple factors [6]. The best characterized inducer of PD-L1 expression in NSCLC is the pro-inflammatory cytokine IFN³, which is secreted by T cells [7,8]. PD-L1 on tumor cells binds to PD-1 on T cells, disrupting T cell function and thereby preventing an effective tumor immune response [9]. Oncogenic driver mutations, such as mutations in EGFR, ALK and BRAF, are known inducers of PD-L1 expression in NSCLC cells. In these oncogene-activated cells, the PI3K/mTOR, JAK/STAT and MAPK pathway are the main drivers of PD-L1 expression [10–13].

Interestingly, EGFR wild-type NSCLC tumors have higher levels of PD-L1 and tumor infiltrating lymphocytes, and respond better to PD-1/PD-L1 targeted therapy compared to EGFR mutant NSCLC [1,2]. However, there are only limited data about the regulation of PD-L1 expression in NSCLC without targetable genetic alterations [14–16]. A better understanding of PD-L1 regulation may provide a rationale to combine immune checkpoint inhibitors with other targeted agents. In the present study, we aimed to identify pathways regulating *CD274* (PD-L1) expression in this NSCLC subtype by using RNA sequencing data from The Cancer Genome Atlas (TCGA) lung adenocarcinoma and squamous cell lung carcinoma data sets. We functionally validated our findings using adenocarcinoma cell lines and cocultures with peripheral blood mononuclear cells (PBMCs). Our results indicate that growth factor-dependent MAPK signaling plays an important role in basal and IFN³-induced PD-L1 expression of lung adenocarcinoma without targetable genetic alterations.

**Methods**

***TCGA data retrieval and analysis***

TCGA RNA sequencing V2 and mutation data for lung adenocarcinoma and squamous cell carcinoma [17,18] were obtained from the cBioportal for Cancer Genomics [19] on October 14th 2018. We selected 230 adenocarcinoma and 178 squamous cell carcinoma samples with complete RNA sequencing and

whole exome sequencing data. Data were analyzed and visualized using R (available from https://www.r-project.org/) and the R studio interface 1.1.453 (available from https://www.rstudio.com/) and ggplot2 package for R 3.5.1 (available from http://ggplot2.tidyverse.org). Our analysis was performed in 159 lung adenocarcinoma and 166 squamous cell lung carcinoma samples without targetable alterations in EGFR, ALK, ROS1, BRAF, ERBB2, MET, or RET [20]. TCGA RNA sequencing data was normalized in two steps. Each expression value was first log10-transformed and next Z-score normalized by subtracting the mean expression of each gene and dividing by the standard deviation. Next, MAPK pathway activation was inferred according to the methods of previously described gene signatures for Rat Sarcoma (RAS) and MEK activation [21,22]. Inferred pathway activities were calculated as described in the original papers. IFN³ signaling was inferred using *IRF1* and *STAT1* mRNA levels, STAT3 signaling by using *STAT3* gene expression. The correlation of *CD274* (PD-L1) mRNA level with these signature scores was calculated using Spearman correlation. To complement this analysis, gene set enrichment analysis (GSEA) was performed on the same samples, using the hallmark PI3K and IFNG signatures in addition to the previously mentioned signatures. Furthermore, we used the C6 oncogenic signaling MEK and EGFR signatures, and an alternative PI3K signature. However, the authors doubt whether their signatures, developed for estrogen receptor positive breast cancer, can  be used for  other tumor types (http://software.broadinstitute.org/gsea/index.jsp, [23,24]). GSEA was performed with 1000 permutations with Z-score normalized *CD274* gene expression as a continuous phenotype label. Genes were ranked based on the Pearson Metric.

## *Cell culture*

The human NSCLC cell lines HCC827, H292, A549, H358 and H460 were obtained from the American Type Culture Collection (ATCC, Manassas, USA). H322 was obtained from Sigma-Aldrich (St Louis, USA). All cell lines are from the adenocarcinoma histological subtype, except H292 which is an adenocarcinoma-like mucoepidermoid carcinoma. Cells were quarantined until screening for microbial contamination and mycoplasma was performed and proven to be negative. Cells were tested and authenticated using short tandem repeat (STR) profiling. Cells were grown in RPMI with 10% FCS, with 2 mM glutamine added for H322 cells. All cells were incubated in a humidified atmosphere with 5% $CO_2$ at 37°C.

## *Antibodies and treatments*

The details of antibodies used for flow cytometry and Western blotting are provided in Supplementary material, Table S1. Western blotting detection was performed using Lumi-Light Western blotting substrate (Roche Diagnostics, Basel, Switzerland). Cells were treated under normal culture conditions

with EGF, HGF, IFN³ (each from R&D Systems, Minneapolis, USA), erlotinib (LC Laboratories, Woburn, USA), cetuximab (Merck KGaA Darmstadt, Germany), selumetinib (AZD6244, Axon Medchem, Reston, USA), XL147 (LC Laboratories), everolimus (Selleckchem Houston, USA), BMS911543 (Selleckchem) and actinomycin D (Sigma-Aldrich).

### *siRNA-transfection*

Cells were transiently transfected with an siRNA targeting *STAT3* (Eurogentec, Liege, Belgium), or a negative control siRNA (12935300, Invitrogen, Carlsbad, USA) using oligofectamine (11252011, Invitrogen) in Opti-MEM (51985, Invitrogen) according to the manufacturer's instructions. Twenty-four hours after transfection, cells were treated with indicated ligands and treatments. After a total of 48 h, STAT3 knockdown efficiency and proteins of interest were analyzed by Western blotting or flow cytometry. All experiments were performed in triplicate.

### *Flow cytometric analysis*

Cells were harvested using trypsin and kept on ice in PBS with 2% FCS during the entire protocol. After harvesting, cells were kept in PBS with 2% FCS until analysis. Cells were incubated with anti-PD-L1 antibodies at 10 µg/mL for 45 minutes. Bound antibody was detected by incubating cells with goat anti-mouse IgG at a 1:50 dilution for 45 minutes. Measurements were performed on a BD Accuri C6 flow cytometer (BD Biosciences, Franklin Lakes, USA). Data analysis was performed with FlowJo v10 (Tree Star, Ashland, USA) and surface receptor expression was expressed as mean fluorescence intensity (MFI). Measurements were corrected for background fluorescence and unspecific binding of the secondary antibody. Unless stated otherwise, all experiments were performed in triplicate.

### *Western blot*

Lysates from cells were made using mammalian protein extraction reagent with protease and phosphatase inhibitors diluted 1:100 (Thermo Fisher Scientific, Waltham, USA). Proteins were separated using SDS-PAGE. Target proteins were detected with the appropriate antibodies and images were captured using a digital imaging system (Bio-Rad, Hercules, USA). All bands were observed around the size specified in Table S2A. Densitometric quantitation of target proteins was calculated using imageJ relative to loading controls ² -actin or GAPDH depending on target protein size (see Supplememtary material Table S2B for data).

*Viability assays*

H292 (8000 cells/well), H358 (20000 cells/well), A549 (2000 cells/well), H322 (10000 cells/well) and H460 (2000 cells/well) cells were plated in 96 well plates in their respective media and after 6 h erlotinib or selumetinib were added in concentrations ranging from 0.01 to 10 µM. After 96 h, cells were fixed in 3.7% formaldehyde and stained using crystal violet. After washing, bound crystal violet was dissolved using 10% ethanoic acid and absorption measured at 590 nm. Cell survival was calculated as percentage of untreated control. All proliferation assays were performed three times in triplicate.

*RNA sample collection and qRT-PCR*

Total RNA was extracted using Trizol reagent (Invitrogen) and possible DNA contamination was removed using TURBO DNase ambion (Life technologies, AM2238). Next, RNA was reverse transcribed to cDNA with M-MLV reverse transcriptase (Thermo Fisher Scientific, 28025013). Real-time PCR was performed using IQ SYBR Green Supermix (Bio-Rad, 1708886) according to manufacturer's instructions. The following primers were used: *CD274* forward 5'-CAATGTGACCAGCACACTGAGAA-3', reverse 5'- GGCATAATAAGATGGCTCCCAGAA-3'; GAPDH forward 5'-CCCACTCCTCCACCTTTGAC-3', reverse 5'-CCACCACCCTGTTGCTGTAG-3'. The relative gene expression was calculated using the double delta CT method and *GAPDH* as loading control [25]. All qPCR experiments were performed three times in duplicate.

*Coculture experiments*

Human PBMCs were isolated from whole blood by Ficoll-Paque density centrifugation (Ficoll-Paque PLUS, GE Healthcare Life Sciences, Marlborough, USA) from peripheral blood donated by healthy volunteers. The acquired PBMCs were activated for 72 h using human T-activator CD3/28 beads (Thermo Fisher Scientific) and 100 IU/mL IL-2 (Proleukin, Novartis, Basel, Switzerland) in the presence of tumor cells. Separately, tumor cells were seeded into 96-well plates at a density of $1 \times 10^4$ cells/well for 48 h. Then, the pre-activated PBMCs were added into the coculture system at a 5:1 ratio of PBMCs to tumor cells. During coculture, cells were treated with EGF (20 ng/mL), erlotinib (10 µM) and selumetinib (10 µM). After 24 h of coculture, cell-free supernatant was collected for IFN³ analysis by ELISA (Sino Biological, Bejing, China). Cells were harvested for flow cytometric measurement of membrane PD-L1. In separate experiments, tumor cells were cultured in cell-free supernatant from activated PBMCs. Membrane PD-L1 levels were determined after 24 h using flow cytometry.

*Statistics*

Cell line experiments were assessed for differences with unpaired two-tailed Student's t-test or two-way ANOVA followed by Bonferroni post-hoc or Dunnett's test. Results are represented as means ± SD. A P-value < 0.05 was considered statistically significant. Statistical analyses were performed using GraphPad Prism software (version 6.0 GraphPad software).

**Results**

***MAPK pathway activation correlates with PD-L1 gene expression in lung adenocarcinoma***

To study which EGFR-related signaling pathways regulate PD-L1 expression in NSCLC without targetable genetic alterations, we collected RNA sequencing data of 159 lung adenocarcinoma and 166 squamous cell lung carcinoma samples from TCGA excluding samples with driver mutations in *EGFR*, *ALK*, *BRAF*, *ROS1*, *MET*, *ERBB2* and *RET*. Activating *KRAS* mutations were present in 75 of the lung adenocarcinoma and 1 of the squamous cell carcinoma samples. Activation of the MAPK pathway was determined using validated signatures for RAS or MEK activation [21,22]. MAPK pathway activation scores were significantly higher in *KRAS* mutant samples (Figure S1A). In addition, there was a moderate correlation between RAS and MEK activation scores (Figure S1B). Interestingly, in adenocarcinomas, but not in squamous cell carcinomas, RAS and MEK activation scores correlated with *CD274* gene expression (Figure 1A, Table 1). Subset analysis showed that these correlations were strongest in *KRAS* wild-type lung adenocarcinomas (Figure 1B, S1C). *STAT3* mRNA levels did not correlate with *CD274* in any subset (Table 1). In both histological subtypes, mRNA levels of *STAT1* and *IRF1*, important mediators of IFN³, correlated with *CD274* (Figure 1C, S1D), *CD8A* ($r_s$ = 0.73, $r_s$ = 0.72), and *IFNG* ($r_s$ = 0.71, $r_s$ = 0.74), respectively. Inferred MEK and RAS activities were not significantly correlated with *STAT1* ($r_s$ 0.12, p = 0.27; $r_s$ 0.1, p = 0.36). Interestingly, a combined score for MAPK and IFN³ signaling, created by adding up 0 to 1 rescaled MEK activation scores and *STAT1* levels, correlated more strongly with *CD274* mRNA levels (Figure S1E). GSEA using RAS, MEK and the Hallmark IFNG signatures largely confirmed these findings. In addition, GSEA of the PI3K hallmark signature suggested a link between PI3K/mTOR signaling and *CD274* (Supplementary material, Table S3). This suggests that activation of the MAPK, PI3K/mTOR, and IFN³ pathway are related to increased *CD274* mRNA levels in lung adenocarcinomas without targetable genetic alterations.

***EGF increases IFN³-induced PD-L1 expression in EGFR wild-type NSCLC cells***

A panel of lung adenocarcinoma cell lines without targetable genetic alterations, including a *KRAS* wild-type (H322), 3 *KRAS* mutant (A549, H358, and H460) and a *KRAS* wild-type adenocarcinoma-like mucoepidermoid carcinoma cell line (H292) [26], was selected to further investigate the relation between EGFR and IFN³ pathway activation with PD-L1 expression. Membrane PD-L1 was observed in all cell lines, irrespective of *KRAS* mutation status (Figure S2A). The highest levels were found in H292, H358 and H460 cells. Levels were comparable to PD-L1 membrane levels of HCC827 *EGFR* mutant NSCLC cells (Figure S2A). We wondered whether IFN³ and EGF, a known activator of the EGFR, PI3K/mTOR and MAPK pathway, would increase PD-L1 levels in our panel. Treatment with EGF or IFN³ for 24 h using physiologically relevant concentrations (20 ng/mL) [27,28] increased membrane PD-L1 in both *KRAS* wild-type and *KRAS* mutant cells (Figure 2A,B). Moreover, exposure of cells to EGF combined with IFN³ resulted in a further increase in PD-L1 compared to IFN³ alone. Prolonged incubation up to 72 h further enhanced PD-L1 in H292 and H358 (Figure 2C).

To gain insight in the underlying mechanism of the increase in surface PD-L1, we measured total PD-L1 protein and *CD274* mRNA levels. The EGF- and IFN³-induced increase in surface expression was reflected in a strong induction of both mRNA and total protein levels (Figure 2D,E). EGF stimulated the MAPK and PI3K/mTOR pathway, as signified by increased levels of phosphorylated ERK 1 and 2 (pERK1/2) and phosphorylated ribosomal S6 protein (pS6), respectively (Figure 2E, S2B). IFN³ strongly increased STAT1 and phosphorylated STAT1 (pSTAT1) levels for up to 72 h. Taken together, these results indicate that EGF and IFN³ activate the MAPK, PI3K/mTOR and STAT1 pathways, and concurrently increase PD-L1 mRNA, protein and membrane levels.


### *EGFR inhibition prevents EGF- and IFN³-induced PD-L1 upregulation*

To analyze the regulation of membrane PD-L1 by EGFR and STAT1 signaling, H292 and H358 cells were treated with EGF and IFN³ in the presence of anti-EGFR monoclonal antibody cetuximab or EGFR small molecule inhibitor erlotinib. Interestingly, cetuximab and erlotinib prevented not only EGF-induced but also IFN³-induced upregulation of *CD274* mRNA levels, which was reflected in reduced membrane and total PD-L1 protein levels (Figure 3A,B; Figure S3A). Data from multiple experiments showed that erlotinib reduced basal PD-L1 membrane levels in H358 but not H292 cells (Figure S3B). Erlotinib had a similar effect on EGF- and IFN³-induced PD-L1 membrane levels in two other cell lines but not in the erlotinib-resistant H460 cell line, as expected (Figure S4A). EGFR inhibition effectively reduced EGF-dependent MAPK and PI3K/mTOR signaling and modestly decreased IFN³-induced upregulation of (p)STAT1 (Figure 3B). These results indicate that EGF- and IFN³-induced *CD274* mRNA, and PD-L1 protein and membrane levels are dependent on EGFR-mediated signaling.

### *MAPK pathway inhibition prevents PD-L1 induction by EGF and IFNᵧ*

Next, we assessed the involvement of MAPK and PI3K/mTOR signaling in PD-L1 upregulation. Selumetinib, an inhibitor of MEK1/2, almost completely suppressed induction of *CD274* mRNA by EGF and IFNᵧ in H292 and H358, and diminished the induction of protein and membrane levels (Figure 4A,B, Figure S3A). Moreover, selumetinib decreased basal PD-L1 membrane levels in H292 and H358 cells (Figure S3B). Selumetinib effectively inhibited MEK1/2 activity, as reflected in the reduction in pERK1/2 levels, and had a moderate effect on pSTAT1 levels. The effect of selumetinib on membrane PD-L1 was confirmed in additional cell lines (Figure S4A). PI3K inhibitor XL147 and mTORC1 inhibitor everolimus partially suppressed EGF- and IFNᵧ-induced PD-L1 in H292 cells, but they had no effect on the induction of membrane PD-L1 (Figure 4A,B). At these concentrations, both drugs effectively inhibited PI3K/mTOR pathway activity, as indicated by reduced pAKT and pS6 levels (Figure 4B).

We pursued studying the MAPK pathway because of its major influence on PD-L1 expression. A wide range of selumetinib and erlotinib concentrations was used to determine if lower drug concentrations also reduce PD-L1 expression. After 24 h even the lowest selumetinib concentration (0.1 µM) strongly reduced pERK levels, as well as PD-L1 protein and membrane expression levels of H292 and H358 cells in both control and EGF- and IFNᵧ-stimulated cells (Figure S3C). Treatment with this selumetinib concentration for 96 h resulted in a growth reduction of 30-50% (Figure S3D), indicating that PD-L1 expression can be manipulated with a MAPK activity inhibitor using concentrations that only partially reduce cell growth. In line with these results, selumetinib had a similar moderate effect on growth in the other three cell lines (Figure S4B). Similar results were observed with erlotinib. Concluding, MAPK pathway inhibitors suppresses EGF- and IFNᵧ-induced *CD274* mRNA, and PD-L1 protein and membrane expression at concentrations that have a small effect on growth.

### *Hepatocyte growth factor induces surface PD-L1 via the MAPK pathway*

We investigated whether activation of the MAPK pathway via hepatocyte growth factor receptor (cMET), has a similar effect on PD-L1 as MAPK activation by EGFR. Overexpression of cMET and its ligand HGF occur frequently in lung adenocarcinoma tumors [29]. Moreover, upon binding of hepatocyte growth factor (HGF), cMET is known to activate PI3K/mTOR, MAPK and JAK/STAT pathways, similar to EGFR [30]. HGF enhanced PD-L1 expression and augmented IFNᵧ-induced PD-L1 expression in the cMET-positive H292 and H358 cell lines (Figure 4C). Combining HGF and EGF had no additional effect on membrane PD-L1 levels compared to single EGF or HGF treatment. Also in this case, selumetinib effectively prevented HGF-induced effects on PD-L1 levels in both cell lines, while erlotinib only showed efficacy in H292 cells. Taken together, these results demonstrate that, irrespective of the upstream growth factor receptor, MAPK pathway activation is essential for PD-L1 membrane expression.

### MAPK pathway inhibition does not interfere with IFN³-induced MHC-I upregulation

Expression of major histocompatibility complex I (MHC-I) is critical for tumor cell antigen presentation and the anti-tumoral immune response [31]. Because both MAPK and IFN³ signaling can influence MHC-I expression, we wondered whether EGFR and MEK1/2 blockade could interfere with its expression in our cell lines [32–34]. IFN³, but not EGF, increased MHC-I membrane expression in 4 out of 5 cell lines (Figure 4D, S4C). Moreover, MAPK pathway inhibition using erlotinib and selumetinib did not influence IFN³-induced upregulation of MHC-I expression, suggesting that MHC-I-mediated tumor cell antigen presentation will not be impaired by these drugs.

### MAPK signaling increases stability of CD274 mRNA

To investigate the role of STAT signaling in MHC-I and PD-L1 expression after IFN³ or EGF treatment, we inhibited STAT1 and STAT3, major transcription factors downstream of IFN³ and EGFR signaling respectively [6,35]. Suppression of STAT1 signaling using JAK2 inhibitor BMS911543 prevented IFN³-induced PD-L1 and MHC-I expression, but not EGF-induced PD-L1 expression (Figure 5A, S5A). Also, inhibition of STAT3 using an siRNA had no influence on PD-L1 regulation by MAPK signaling (Figure S5B). Therefore, we hypothesized that the MAPK pathway may regulate PD-L1 at a posttranscriptional level. *KRAS* mutations were recently shown to be involved in posttranscriptional regulation of basal PD-L1 levels through modulation of *CD274* mRNA stability [36]. To study whether MAPK signaling controls stability of IFN³-induced *CD274* mRNA, *KRAS* wild-type and mutant cells were pretreated with IFN³ followed by the addition of the transcriptional blocker actinomycin D [37]. Blocking transcription for 90 minutes halved *CD274* levels (Figure 5B). Interestingly, degradation of *CD274* was counteracted by EGF-induced activation of MAPK signaling. Accordingly, inhibition of MAPK signaling with selumetinib accelerated *CD274* degradation and decreased the stabilization by EGF. These results show that MAPK signaling influences stability of *CD274* mRNA, contributing to regulation of PD-L1 protein and membrane expression.

### MAPK pathway inhibition decreases PBMC-induced PD-L1 surface expression

To study the relation between immune cell activation and PD-L1 expression of tumor cells, we performed cocultures of PBMCs and NSCLC cells. After 24 h coculture, membrane PD-L1 and MHC-I were strongly induced in tumor cells (Figure 6A, B). Conditioned medium from activated PBMCs contained IFN³ (30 ng/mL) in comparable levels to our other experiments and also strongly induced membrane PD-L1, indicating IFN³ may be involved in PBMC-induced PD-L1 (Figure S6A,B). Similar to our previous

experiments, EGF further enhanced tumor cell MAPK pathway activity and PD-L1 expression, which was counteracted by erlotinib and selumetinib, without influencing MHC-I (Figure 6A,B, S6A). Our results indicate that MAPK pathway inhibition can reduce tumor cell PD-L1 in a more complex coculture system, without interfering with MHC-I induction in tumor cells, potentially improving immunogenicity of these cells.

**Discussion**

In this study we revealed a correlation between MAPK pathway activation and *CD274* expression in lung adenocarcinomas without targetable genetic alterations using TCGA RNA sequencing data. Subsequently, we demonstrated the importance of MAPK signaling in the upregulation of PD-L1 by growth factors and IFN³ in lung adenocarcinoma cell lines, which was mediated through *CD274* mRNA stability and STAT1 activation (Figure 6C). Inhibition of the MAPK pathway prevents growth factor-, IFN³-, and PBMC-induced PD-L1 upregulation, whereas it does not interfere with MHC-I expression. Taken together, these results indicate that MAPK pathway inhibition may improve tumor cell immunogenicity of lung adenocarcinomas without targetable genetic alterations, comprising almost 60% of all lung adenocarcinoma tumors in the Western world [3].

Our TCGA analysis suggests MAPK pathway activity and *CD274 g*ene expression are primarily connected in lung adenocarcinoma, but not in squamous cell carcinoma of the lung. Targeting the MAPK pathway is especially interesting in lung adenocarcinoma, because these tumors have a more active MAPK pathway and more frequently harbor *KRAS* mutations compared to squamous cell carcinoma tumors [38,39]. Intriguingly, this is also the subtype where tumor cell PD-L1 has predictive and prognostic value [40,41]. Our study shows that MAPK pathway inhibition prevents the induction of *CD274* mRNA by EGF and IFN³ through two separate mechanisms (Figure 6C). Firstly, a moderate dose-dependent reduction of STAT1 and pSTAT1 levels upon inhibition of EGFR or MEK1/2 may lower *CD274* transcription (Figure S3C). This might be due to the inhibition of the eukaryotic initiation factor 4F (eIF4F) translation initiation complex, which is a downstream effector of the MAPK pathway and essential for cap-dependent translation of *STAT1* [39,42]. Secondly, we observed reduced *CD274* mRNA stability upon inhibition of MEK1/2 or EGFR. This expands earlier data on basal PD-L1 expression in *KRAS* mutant cell lines, where MEK1/2 inhibition activates tristetraprolin (TTP), resulting in *CD274* mRNA degradation [36]. Although *CD274* transcription and MHC-I-related transcription are both regulated by STAT1 [6,35], MAPK inhibition, in contrast to JAK2 inhibition, does not affect MHC-I expression, suggesting that MAPK activity primarily regulates *CD274* mRNA stability in lung adenocarcinoma cells. At the protein level, PD-L1 can be affected by several mechanisms such as glycosylation, ubiquitination and stabilization at the cell membrane [15,43–45]. However, we found no direct effect of EGF or IFN³ on CKLF-like MARVEL transmembrane domain containing protein 6 (CMTM6) protein levels in H292 or H358 cells (data not shown).

Our experiments demonstrated that both EGFR and MEK1/2 inhibitors decrease EGF- and IFN³-induced PD-L1 expression, potentially increasing immunogenicity of lung adenocarcinoma cells. Nevertheless, because the MAPK pathway is downstream of a plethora of growth factor receptors, downstream inhibition with MEK1/2 inhibitors may be more effective to modulate PD-L1 than inhibition of specific growth factor receptors. This is supported by our finding that MEK1/2 inhibition, but not EGFR inhibition, prevented HGF-induced PD-L1 expression and by earlier findings in renal cell carcinoma [46]. *In vitro* we observed PD-L1 downregulation at selumetinib concentrations that had a small effect on cell growth. Although *in vitro* experiments do not perfectly model the tumor microenvironment, our results suggest that an immunomodulatory effect may already be present at lower selumetinib doses than previously utilized in NSCLC patients [47,48]. The immunomodulatory role of MAPK signaling is increasingly being recognized [49]. Multiple studies using *in vivo* colon cancer models showed that MEK inhibition potentiates the anti-tumor immune response by preventing T cell apoptosis and decreasing levels of myeloid suppressor cells and regulatory T cells. This resulted in sustained tumor regression when combined with PD-L1, PD-1, or cytotoxic T-lymphocyte-associated protein 4 (CTLA-4) blocking treatment [50–52]. In phase II and III studies of selumetinib in NSCLC patients, disappointing efficacy was observed [47,48]. However, clear immune modulating effects were observed, indicating that MAPK pathway inhibition may increase the efficacy of immunotherapy. Modulating PD-L1 expression is especially interesting in NSCLC tumors without targetable genetic alterations, because these have a more inflamed tumor microenvironment and respond better to immune checkpoint inhibitors than tumors with targetable genetic alterations, such as EGFR mutations [1,2]. These combination strategies are currently being tested in NSCLC patients (NCT03600701, NCT03299088).

In conclusion, our results show the importance of growth factor induced MAPK pathway signaling in PD-L1 expression in lung adenocarcinoma without targetable genetic alterations. This provides a rationale to explore the combination of MAPK pathway inhibitors with immunotherapy in this lung cancer subtype.

### Author contributions

TS, AK, AT, and SJ designed, performed and interpreted the experiments. EV gave valuable input on structuring the experiments; MB and RF respectively guided the coculture and in silico experiments. TS

and AK wrote the manuscript and put the figures together; EV, MB, RF, AT, and SJ made revisions and proofread the manuscript. All authors read and approved the final manuscript.

**List of abbreviations**

CMTM6, CKLF-like MARVEL transmembrane domain containing protein 6; CTLA-4, cytotoxic T-lymphocyte-associated protein 4; ELISA, enzyme-linked immunosorbent assay; GSEA, gene set enrichment analysis; IFNɣ, interferon ɣ; IRF1, interferon regulatory factor 1; LUSC, squamous cell lung carcinoma; MFI, mean fluorescence intensity; mTOR, mammalian target of rapamycin; NSCLC, non-small cell lung cancer; PBMC, peripheral blood mononuclear cell; PD-1, programmed cell death protein 1; PD-L1, programmed death-ligand 1; siRNA, small interfering RNA; TCGA, The Cancer Genome Atlas.

**Supplementary material online**

**Supplementary methods - NO**

**Supplementary Figure legends NO (legends are contained within the figures)**

**Figure S1**. Supplementary TCGA analyses

**Figure S2.** EGF and IFNɣ increase PD-L1 expression in EGFR and ALK wild-type lung adenocarcinoma cell lines

**Figure S3.** MAPK pathway inhibition decreases EGF- and IFNɣ-induced PD-L1 expression at non-toxic concentrations.

**Figure S4.** Effects of MAPK pathway inhibition on PD-L1 and MHC-I expression and proliferation in a panel of NSCLC cell lines.

**Figure S5.** JAK2 and STAT3 influence MHC-I, but not PD-L1 signaling

**Figure S6.** PBMC-derived IFNɣ may play a role in PD-L1 induction.

**Table S1.** Antibodies used in the study

**Table S2.** (A) Molecular weight Western blot proteins. (B) Densitometric quantitations of all Western blots in the study

**Table S3.** GSEA results

## References

1    Dong ZY, Zhang JT, Liu SY, *et al.* EGFR mutation correlates with uninflamed phenotype and weak immunogenicity, causing impaired response to PD-1 blockade in non-small cell lung cancer. *Oncoimmunology* 2017; **6**: e1356145.

2    Zhang M, Li G, Wang Y, *et al.* PD-L1 expression in lung cancer and its correlation with driver mutations: a meta-analysis. *Sci Rep* 2017; **7**: 10255.

3    Hirsch FR, Scagliotti G V., Mulshine JL, *et al.* Lung cancer: current therapies and new targeted treatments. *Lancet* 2017; **389**: 299-311.

4    Sacher AG, Gandhi L. Biomarkers for the clinical use of PD-1/PD-L1 inhibitors in non-small-cell lung cancer: A review. *JAMA Oncol* 2016; **2**: 1217-1222.

5    Ferrara R, Mezquita L, Besse B. Progress in the management of advanced thoracic malignancies in 2017. *J Thorac Oncol* 2018; **13**: 301-322.

6    Sun C, Mezzadra R, Schumacher TN. Regulation and function of the PD-L1 checkpoint. *Immunity* 2018; **48**: 434-452.

7    Lee S-J, Jang B-C, Lee S-W, *et al.* Interferon regulatory factor-1 is prerequisite to the constitutive expression and IFN-gamma-induced upregulation of B7-H1 (CD274). *FEBS Lett* 2006; **580**: 755-762.

8    Schalper KA, Carvajal-Hausdorf D, McLaughlin J, *et al.* Differential expression and significance of PD-L1, IDO-1, and B7-H4 in human lung cancer. *Clin Cancer Res* 2017; **23**: 370-378.

9    Califano R, Kerr K, Morgan RD, *et al.* Immune checkpoint blockade: a new era for non-small cell lung cancer. *Curr Oncol Rep* 2016; **18**: 59.

10    Chen N, Fang W, Zhan J, *et al.* Upregulation of PD-L1 by EGFR activation mediates the immune escape in EGFR-driven NSCLC: implication for optional immune targeted therapy for NSCLC patients with EGFR mutation. *J Thorac Oncol* 2015; **10**: 910-923.

11    Ota K, Azuma K, Kawahara A, *et al.* Induction of PD-L1 expression by the EML4-ALK oncoprotein and downstream signaling pathways in non-small cell lung cancer. *Clin Cancer Res* 2015; **21**: 4014-4021.

12    Concha-Benavente F, Srivastava RM, Trivedi S, *et al.* Identification of the cell-intrinsic and -extrinsic pathways downstream of EGFR and IFN³ that induce PD-L1 expression in head and neck cancer. *Cancer Res* 2016; **76**: 1031-1043.

13    Sumimoto H, Takano A, Teramoto K, *et al.* RAS-mitogen-activated protein kinase signal is required for enhanced PD-L1 expression in human lung cancers. *PLoS One* 2016; **11**: e0166626.

14    Li C-W, Lim S-O, Xia W, *et al.* Glycosylation and stabilization of programmed death ligand-1 suppresses T-cell activity. *Nat Commun* 2016; **7**: 12632.

15    Horita H, Law A, Hong S, *et al.* Identifying regulatory posttranslational modifications of PD-L1: a focus on monoubiquitination. *Neoplasia* 2017; **19**: 346-353.

16    Lastwika KJ, Wilson W, Li QK, *et al.* Control of PD-L1 expression by oncogenic activation of the AKT-mTOR pathway in non-small cell lung cancer. *Cancer Res* 2016; **76**: 227-238.

17    Imielinski M, Berger AH, Hammerman PS, *et al.* Mapping the hallmarks of lung adenocarcinoma with massively parallel sequencing. *Cell* 2012; **150**: 1107-1120.

18    Network TCGAR. Comprehensive genomic characterization of squamous cell lung cancers. *Nature* 2014; **489**: 519-525.

19    Cerami E, Gao J, Dogrusoz U, *et al.* The cBio cancer genomics portal: an open platform for exploring multidimensional cancer genomics. *Cancer Discov* 2012; **2**: 401-404.

20    National Comprehensive Cancer Network. Non-small cell lung cancer (Version 11.2019). https://www.nccn.org/professionals/physician_gls/pdf/nscl.pdf. Accessed January 2019.

21    Dry JR, Pavey S, Pratilas CA, *et al.* Transcriptional pathway signatures predict MEK addiction and response to selumetinib (AZD6244). *Cancer Res* 2010; **70**: 2264-2273.

22    Loboda A, Nebozhyn M, Klinghoffer R, *et al.* A gene expression signature of RAS pathway dependence predicts response to PI3K and RAS pathway inhibitors and expands the population of RAS pathway activated tumors. *BMC Med Genomics* 2010; **3**: 26.

23    Creighton CJ, Fu X, Hennessy BT, *et al.* Proteomic and transcriptomic profiling reveals a link between the PI3K pathway and lower estrogen-receptor (ER) levels and activity in ER+ breast cancer. *Breast Cancer Res* 2010; **12**: R40.

24    Creighton CJ, Hilger AM, Murthy S, *et al.* Activation of mitogen-activated protein kinase in estrogen receptor alpha-positive breast cancer cells in vitro induces an in vivo molecular phenotype of estrogen receptor alpha-negative human breast tumors. *Cancer Res* 2006; **66**: 3903-3911.

25    Livak KJ, Schmittgen TD. Analysis of relative gene expression data using real-time quantitative PCR and the 2-"" CT method. *Methods* 2001; **25**: 402-408.

26    Wang R, Li Y, Hu E, *et al.* S100A7 promotes lung adenocarcinoma to squamous carcinoma transdifferentiation, and its expression is differentially regulated by the Hippo-YAP pathway in lung cancer cells. 2017; **8**: 24804-24814.

27    Sigismund S, Woelk T, Puri C, *et al.* Clathrin-independent endocytosis of ubiquitinated cargos. *Proc Natl Acad Sci U S A* 2005; **102**: 2760-2765.

28    Qin A, Coffey DG, Warren EH, *et al.* Mechanisms of immune evasion and current status of checkpoint inhibitors in non-small cell lung cancer. *Cancer Med* 2016; **5**: 2567-2578.

29    Matsumura Y, Umemura S, Ishii G, *et al.* Expression profiling of receptor tyrosine kinases in high-grade neuroendocrine carcinoma of the lung: a comparative analysis with adenocarcinoma and squamous cell carcinoma. *J Cancer Res Clin Oncol* 2015; **141**: 2159-2170.

30    Gelsomino F, Facchinetti F, Haspinger ER, *et al.* Targeting the MET gene for the treatment of non-small-cell lung cancer. *Crit Rev Oncol Hematol* 2014; **89**: 284-299.

31    Leone P, Shin E-C, Perosa F, *et al.* MHC class I antigen processing and presenting machinery: organization, function, and defects in tumor cells. *J Natl Cancer Inst* 2013; **105**: 1172-1187.

32    Brea EJ, Oh CY, Manchado E, *et al.* Kinase regulation of human MHC class I molecule expression on cancer cells. *Cancer Immunol Res* 2016; **4**: 936-947.

33    Mimura K, Kua L-F, Shiraishi K, *et al.* Inhibition of mitogen-activated protein kinase pathway can induce upregulation of human leukocyte antigen class I without PD-L1-upregulation in contrast to interferon-³ treatment. *Cancer Sci* 2014; **105**: 1236-1244.

34    Im JS, Herrmann AC, Bernatchez C, *et al.* Immune-modulation by epidermal growth factor receptor inhibitors: implication on anti-tumor immunity in lung cancer. *PLoS One* 2016; **11**: e0160004.

35    Zhou F. Molecular mechanisms of IFN-gamma to up-regulate MHC class I antigen processing and presentation. *Int Rev Immunol* 2009; **28**: 239-260.

36    Coelho MA, de Carné Trécesson S, Rana S, *et al.* Oncogenic RAS signaling promotes tumor immunoresistance by stabilizing PD-L1 mRNA. *Immunity* 2017; **47**: 1083-1099.e6.

37    Bensaude O. Inhibiting eukaryotic transcription: Which compound to choose? How to evaluate its activity? *Transcription* 2011; **2**: 103-108.

38    Fumarola C, Bonelli MA, Petronini PG, *et al.* Targeting PI3K/AKT/mTOR pathway in non small cell lung cancer. *Biochem Pharmacol* 2014; **90**: 197-207.

39    Yoshizawa A, Fukuoka J, Shimizu S, *et al.* Overexpression of phospho-eIF4E is associated with survival through AKT pathway in non-small cell lung cancer. 2010; **16**: 240-249.

40    Brahmer J, Reckamp KL, Baas P, *et al.* Nivolumab versus docetaxel in advanced squamous-cell non-small-cell lung cancer. *N Engl J Med* 2015; **373**: 123-135.

41    Borghaei H, Paz-Ares L, Horn L, *et al.* Nivolumab versus docetaxel in advanced nonsquamous non-small-cell lung cancer. *N Engl J Med* 2015; **373**: 1627-1639.

42    Cerezo M, Guemiri R, Druillennec S, *et al.* Translational control of tumor immune escape via the eIF4F-STAT1-PD-L1 axis in melanoma. *Nat Med* 2018; **24:** 1877-1886.

43    Mezzadra R, Sun C, Jae LT, *et al.* Identification of CMTM6 and CMTM4 as PD-L1 protein regulators. *Nature* 2017; **549**: 106-110.

44    Burr ML, Sparbier CE, Chan YC, *et al.* CMTM6 maintains the expression of PD-L1 and regulates anti-tumour immunity. *Nature* 2017; **549**: 101-105.

45    Li CW, Lim S., Chung EM, *et al.* Eradication of triple-negative breast cancer cells by targeting glycosylated PD-L1. *Cancer Cell* 2018; **33**: 187-201.e10.

46    Balan M, Mier y Teran E, Waaga-Gasser AM, *et al.* Novel roles of c-Met in the survival of renal cancer cells through the regulation of HO-1 and PD-L1 expression. *J Biol Chem* 2015; **290**: 8110-8120.

47    Jänne PA, van den Heuvel MM, Barlesi F, *et al.* Selumetinib plus docetaxel compared with docetaxel alone and progression-free survival in patients with KRAS-mutant advanced non-small cell lung cancer: the SELECT-1 randomized clinical trial. *JAMA* 2017; **317**: 1844-1853.

48    Carter CA, Rajan A, Keen C, *et al.* Selumetinib with and without erlotinib in KRAS mutant and KRAS wild-type advanced nonsmall-cell lung cancer. *Ann Oncol* 2016; **27**: 693-699.

49    Bedognetti D, Roelands J, Decock J, *et al.* The MAPK hypothesis: immune-regulatory effects of MAPK-pathway genetic dysregulations and implications for breast cancer immunotherapy. *Emerg Top Life Sci* 2017; **1**: 429-445.

50    Liu L, Mayes PA, Eastman S, *et al.* The BRAF and MEK inhibitors dabrafenib and trametinib: effects on immune function and in combination with immunomodulatory antibodies targeting PD-1, PD-L1, and CTLA-4. *Clin Cancer Res* 2015; **21**: 1639-1651.

51    Poon E, Mullins S, Watkins A, *et al.* The MEK inhibitor selumetinib complements CTLA-4 blockade by reprogramming the tumor immune microenvironment. *J Immunother cancer* 2017; **5**:

63.

52    Ebert PJR, Cheung J, Yang Y, *et al.* MAP kinase inhibition promotes T cell and anti-tumor
      activity in combination with PD-L1 checkpoint blockade. *Immunity* 2016; **44**: 609-621.

**Table 1.** Correlation between inferred MAPK, PI3K/mTOR and IFN³ pathway activity, and PD-L1 gene expression in NSCLC subtypes

| | | Adenocarcinoma | | | EGFRmt | LUSC |
| --- | --- | --- | --- | --- | --- | --- |
| | | Non-targetable | | | | Non-targetable |
| | | Total $n = 159$ | KRASmt $n = 73$ | KRASwt $n = 86$ | Total $n = 28$ | KRASwt $n = 166$ |
| **RAS-score** | $r_s$ | 0.42 | 0.32 | 0.47 | 0.52 | -0.06 |
| | p | $4.1 \times 10^{-8}$ | 0.006 | $7.6 \times 10^{-6}$ | 0.005 | ns |
| **MEK-score** | $r_s$ | 0.40 | 0.21 | 0.51 | 0.13 | 0.04 |
| | p | $2.0 \times 10^{-7}$ | ns | $7.5 \times 10^{-7}$ | ns | ns |
| **STAT3** | $r_s$ | -0.15 | -0.20 | -0.10 | -.08 | 0.11 |
| | p | ns | ns | ns | ns | ns |
| **STAT1** | r | 0.54 | 0.66 | 0.48 | 0.33 | 0.43 |
| | p | $< 2.2 \times 10^{-16}$ | $< 2.2 \times 10^{-16}$ | $4.9 \times 10^{-6}$ | ns | $1.6 \times 10^{-8}$ |
| **IRF1** | r | 0.49 | 0.43 | 0.53 | 0.47 | 0.33 |
| | p | $8.8 \times 10^{-11}$ | $2.0 \times 10^{-4}$ | $2.0 \times 10^{-7}$ | 0.01 | $2.1 \times 10^{-5}$ |

wt = wild-type; mt = mutant; $r_s$ = Spearman's rho; ns = not significant

**Figure legends**

**Figure 1.** MAPK and IFN³ signaling correlate with PD-L1 expression in lung adenocarcinoma tumors without targetable genetic alterations. RNA sequencing data from all TCGA lung adenocarcinoma and squamous cell lung carcinoma samples without targetable genetic alterations was collected. RNA sequencing data were Z-score normalized after $^{10}$log transformation. (A) Spearman correlation between *CD274* and RAS-activation score or MEK-activation score in all samples. (B) Spearman correlation between *CD274* expression and RAS-activation score or MEK-activation score in *KRAS* wild-type lung adenocarcinoma samples. (C) Spearman correlation between *STAT1* and *CD274* in all samples. LUSC = squamous cell lung carcinoma.

**Figure 2.** EGF and IFN³ induce PD-L1 in NSCLC cell lines**.** (A, B) NSCLC cell lines without targetable genetic alterations treated with 20 ng/mL EGF, 20 ng/mL IFN³, or both. After 24 h, PD-L1 membrane expression was measured using flow cytometry (Student's t test; ns = not significant, * P < 0.05, ** P < 0.01 compared to IFN³, n = 3-11, combined data from all other figures). (C) Membrane PD-L1 levels measured using flow cytometry in cells treated with EGF and IFN³ for 24 or 72 h. Data are represented as MFI / mean corresponding control MFI, n = 3). (D) PD-L1 mRNA levels measured using RT-qPCR on H292 and H358 treated with 20 ng/mL EGF or IFN³, or both for 24 h. Data were analyzed using the double delta CT method and GAPDH as loading control. (E) Western blotting of protein extracts from H292 and H358 treated with 20 ng/mL EGF, 20 ng/mL IFN³, or both, for 1, 24, 48, and 72 h. Actin was used as loading control. Con = untreated control.

**Figure 3.** EGFR inhibition prevents EGF- and IFN³-induced PD-L1 expression. H292 and H358 cells were treated with 20 µg/mL cetuximab or 10 µM erlotinib with and without co-treatment with 20 ng/mL EGF, 20 ng/mL IFN³, or both, for 24 h. (A) Membrane PD-L1 measured using flow cytometry (two-way ANOVA with Dunnett's multiple comparisons test; ** P < 0.01, *** P < 0.001 compared to untreated control). (B) Cellular protein levels measured using Western blotting. Actin was used as loading control. Data from a representative experiment are shown. C = untreated control, E + I = EGF + IFN³.

**Figure 4.** Selumetinib effectively decreases growth factor- and IFN³-induced PD-L1 expression. H292 and H358 cells were treated with 10 µM XL147, 10 µM everolimus, or 10 µM selumetinib, with and without co-treatment with 20 ng/mL EGF, 20 ng/mL IFN³, or both for 24 h. (A) Flow cytometry of membrane PD-L1 (two-way ANOVA with Dunnett's multiple comparisons test, * P < 0.05, *** P < 0.001 compared to ligand-stimulated control). (B) Western blotting of cellular protein levels. Actin was used as loading control. Data are from a representative experiment (n = 2). (C) Membrane PD-L1 and (D)

MHC-1 levels measured by flow cytometry of H292 and H358 cells treated with 10 µM erlotinib or 10 µM selumetinib, with and without co-treatment with 20 ng/mL EGF, 20 ng/mL HGF, 20 ng/mL IFN³, or a combination, for 24 h. In (C), two-way ANOVA with Dunnett's multiple comparisons test * P < 0.05, ** P < 0.01, *** P < 0.001 compared to ligand-stimulated control). (D) Student's t test ** P < 0.01. ns = not significant, C = untreated control, XL = XL147, Ev = everolimus, Selu = selumetinib. H+E+I = HGF + EGF + IFN³.

**Figure 5.** MAPK signaling increases PD-L1 mRNA stability. (A) Membrane PD-L1 using flow cytometry and cellular protein levels by Western blotting in cells treated with BMS911543 in the presence of 20 ng/mL EGF and IFN³ for 24 h. Blot from a representative experiment (n = 2). (B) RT-qPCR of *CD274* mRNA levels (PD-L1) in H292 and H358 cells initially treated with IFN³ for 24 h, then with 5 µg/mL actinomycin D for 10 minutes, followed by 20 ng/mL IFN³, 20 ng/mL EGF, or 10µM selumetinib for 80 minutes. Data were analyzed using the double delta CT method and GAPDH as a loading control (two-way ANOVA with Tukey test * P < 0.05, ** P < 0.01, *** P < 0.001). Con = untreated control, E+I = EGF + IFN³, ActD = actinomycin D.

**Figure 6.** Erlotinib and selumetinib prevent PBMC-induced PD-L1, but not MHC-I expression in NSCLC cells. (A) H292 and H358 cells were cocultured with 72 h pre-activated PBMCs from healthy volunteers at a ratio of 5 PBMCs per tumor cell. During coculture, cells were treated with 20 ng/mL EGF, and 10 µM erlotinib or 10 µM selumetinib. Membrane PD-L1 was measured by flow cytometry after 24 h (two-way ANOVA with Bonferroni's multiple comparisons method ** P < 0.01, *** P < 0.01 compared to control + pre-activated PBMCs). (B) Membrane MHC-I measured using flow cytometry (Two-way ANOVA * P < 0.05, ** P < 0.01 compared to control). R = resting PBMCs, A = activated PBMCs. (C) Proposed model for the role of IFN³ and MAPK signaling in PD-L1 regulation in lung adenocarcinoma. IFN³ derived from tumor infiltrating immune cells induces transcription of PD-L1 in tumor cells through activation of JAK/STAT-signaling. PD-L1 mRNA is translated into PD-L1 protein, which is transported to the cell membrane. Growth receptor- and KRAS mutation-induced MAPK signaling increases STAT signaling, potentially adding to transcriptional activity. Also, MAPK signaling increases stability of PD-L1 mRNA, resulting in increased mRNA and protein levels, and subsequently increasing PD-L1 membrane expression.
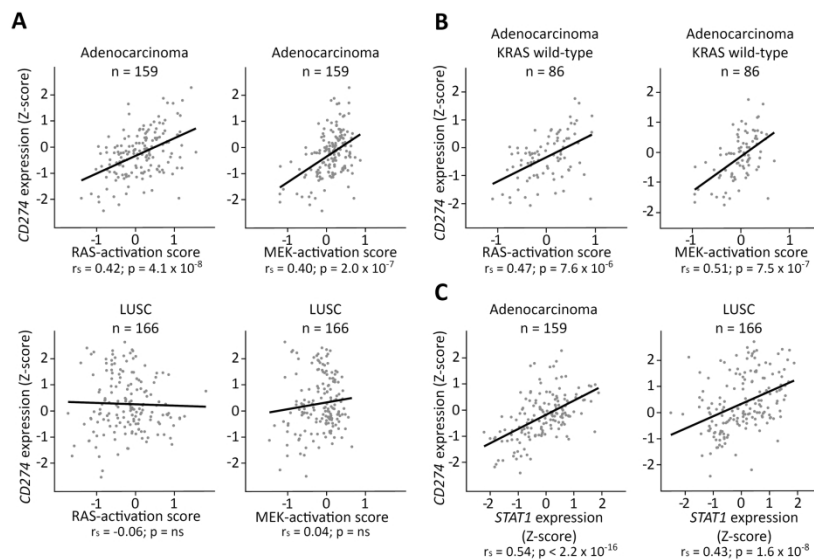
Figure 1. MAPK and IFNγ signaling correlate with PD-L1 expression in lung adenocarcinoma tumors without targetable genetic alterations. RNA sequencing data from all TCGA lung adenocarcinoma and squamous cell lung carcinoma samples without targetable genetic alterations was collected. RNA sequencing data was Z-score normalized after 10log transformation. (A) In all samples the correlation between CD274 expression and RAS-activation score or MEK-activation score was calculated using Spearman correlation. (B) In the KRAS wild-type lung adenocarcinoma samples, the correlation between CD274 expression and RAS-activation score or MEK-activation score was calculated using Spearman correlation. (C) In all collected samples, the correlation between STAT1 and CD274 expression was calculated using Spearman correlation. LUSC = squamous cell lung carcinoma.
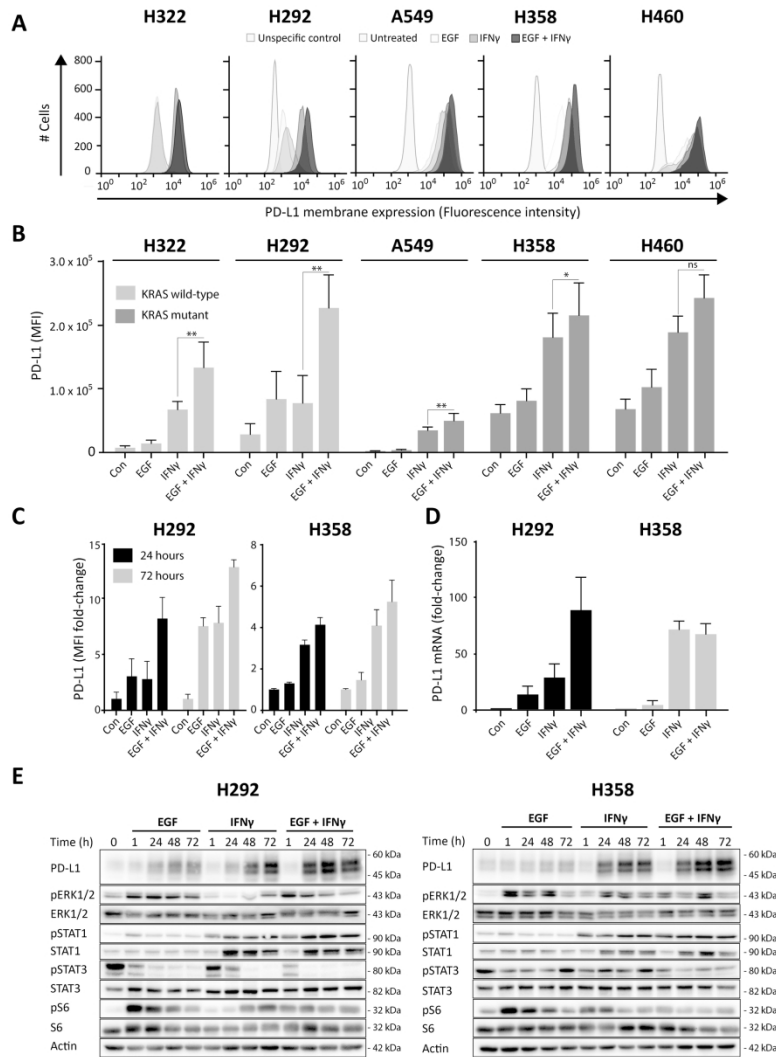
209x297mm (300 x 300 DPI)

Figure 2. EGF and IFNγ induce PD-L1 in NSCLC cell lines. (A, B) A panel of NSCLC cell lines without targetable genetic alterations was treated with 20 ng/mL EGF, 20 ng/mL IFNγ, or both. After 24 hours, PD-L1 membrane expression was measured using flow cytometry. (Student's t test ns = not significant, * P < 0.05, ** P < 0.01 compared to IFNγ, n = 3-11, combined data from all other figures). (C) Cells were treated with EGF and IFNγ for 24 or 72 hours. PD-L1 membrane expression was measured using flow cytometry. (Represented as MFI / mean corresponding control MFI, n = 3) (D) H292 and H358 were treated with 20 ng/mL EGF or IFNγ, or both. After 24 hours PD-L1 mRNA levels were measured using RT-qPCR. Data was analyzed using the double delta CT method and GAPDH as a loading control. (E) H292 and H358 were treated with 20 ng/mL EGF, 20 ng/mL IFNγ, or both. After 1, 24, 48, and 72 hours, protein levels were measured using Western blotting. Actin was used as loading control. Con = untreated control.
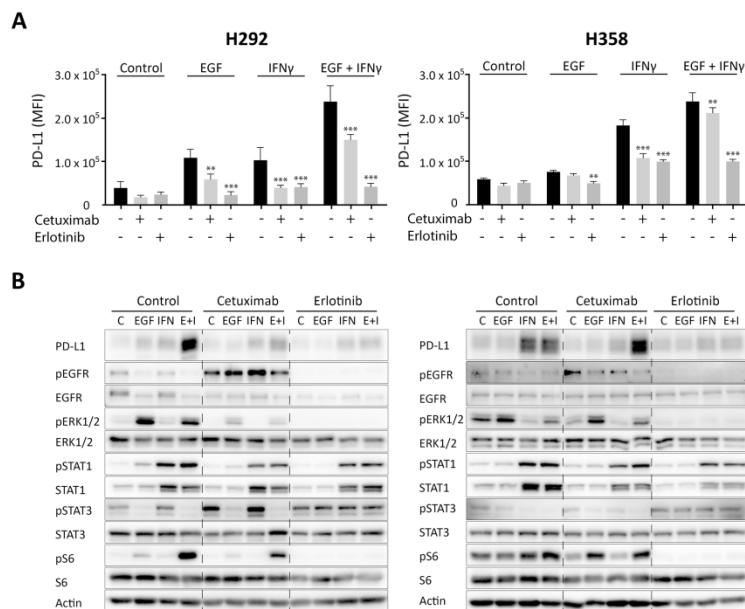
209x297mm (300 x 300 DPI)

Figure 3. EGFR inhibition prevents EGF- and IFNγ-induced PD-L1 expression. H292 and H358 cells were treated with 20 µg/mL cetuximab or 10 µM erlotinib with and without co-treatment with 20 ng/mL EGF, 20 ng/mL IFNγ, or both. (A) After 24 hours, PD-L1 membrane expression was measured using flow cytometry. (Two-way ANOVA with Dunnett's multiple comparisons test ** P < 0.01, *** P < 0.001 compared to untreated control). (B) After 24 hours cellular protein levels were measured using Western blotting. Actin was used as loading control. Data from a representative experiment are shown. C = untreated control, E + I = EGF + IFNγ.
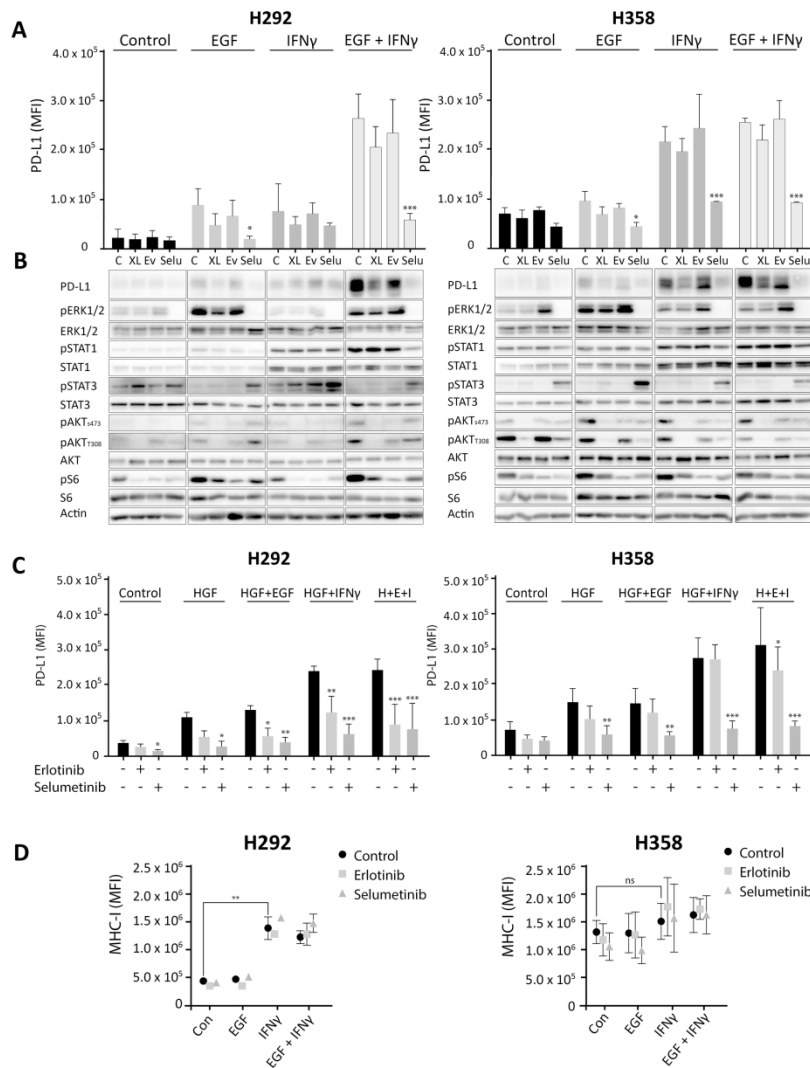
209x297mm (300 x 300 DPI)

Figure 4. Selumetinib effectively decreases growth factor- and IFNγ-induced PD-L1 expression. H292 and H358 cells were treated with 10 μM XL147, 10 μM everolimus, or 10 μM selumetinib, with and without co-treatment with 20 ng/mL EGF, 20 ng/mL IFNγ, or both. (A) After 24 hours, PD-L1 membrane expression was measured using flow cytometry. (Two-way ANOVA with Dunnett's multiple comparisons test, * P < 0.05, *** P < 0.001 compared to ligand-stimulated control) (B) After 24 hours, cellular protein levels were measured using Western blotting. Actin was used as loading control. Data are from a representative experiment. N = 2. (C) H292 and H358 cells were treated with 10 μM erlotinib or 10 μM selumetinib, with and without co-treatment with 20 ng/mL EGF, 20 ng/mL HGF, 20 ng/mL IFNγ, or a combination. After 24 hours, PD-L1 tumor cell membrane expression was measured using flow cytometry. (Two-way ANOVA with Dunnett's multiple comparisons test * P < 0.05, ** P < 0.01, *** P < 0.001 compared to ligand-stimulated control). (D) Cells were treated with 10 μM selumetinib or 10 μM erlotinib with and without co-treatment with 20 ng/mL EGF, 20 ng/mL IFNγ, or both. After 24 hours, MHC-I expression was measured using flow cytometry (Student's t test ** P < 0.01). ns = not significant, C = untreated control, XL = XL147, Ev = everolimus, Selu = selumetinib. H+E+I = HGF + EGF + IFNγ
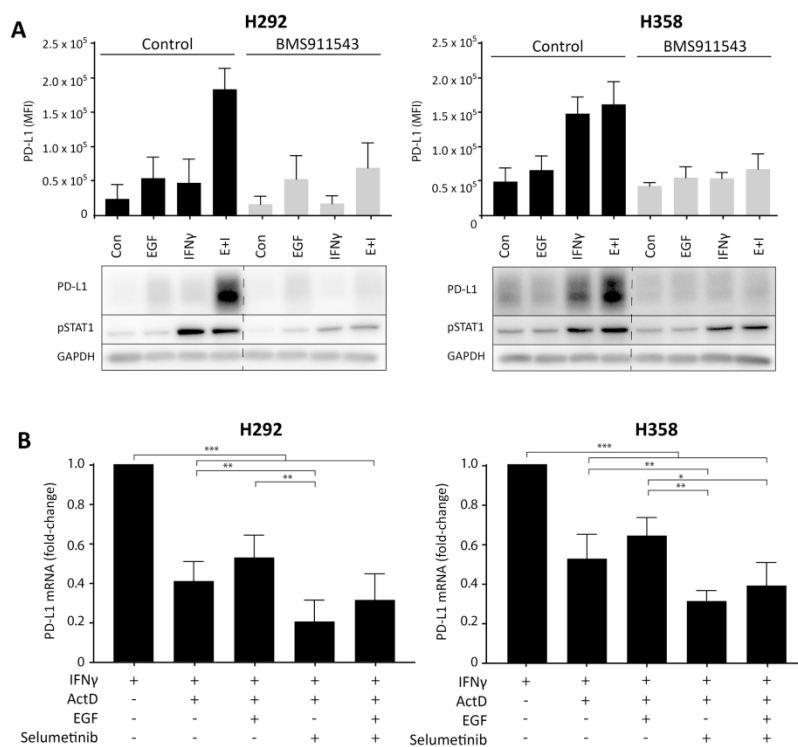
Figure 5. MAPK signaling increases PD-L1 mRNA stability. (A) Cells were treated with BMS911543 in the presence of 20 ng/mL EGF and IFNγ. After 24 hours PD-L1 membrane expression was measured using flow cytometry and cellular protein levels were measured using Western blotting. Blot from a representative experiment. N = 2. (B) H292 and H358 were treated with IFNγ for 24 hours. After washing, cells were treated with 5 μg/mL actinomycin for 10 minutes, after which 20 ng/mL IFNγ, 20 ng/mL EGF, or 10μM selumetinib were added for 80 minutes. RNA was harvested and PD-L1 mRNA levels were measured using RT-qPCR. Data was analyzed using the double delta CT method and GAPDH as a loading control. (Two-way ANOVA with Tukey test * P < 0.05, ** P < 0.01, *** P < 0.001). Con = untreated control, E+I = EGF + IFNγ, ActD = actinomycin D.
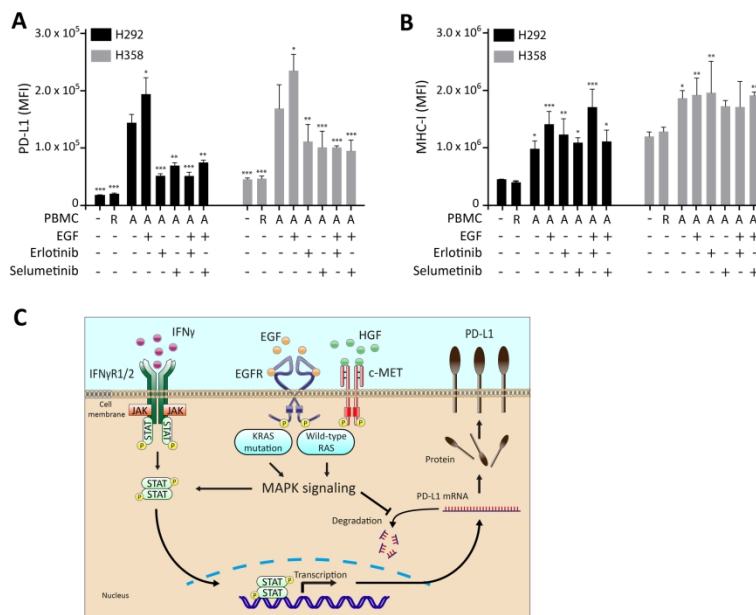
209x297mm (300 x 300 DPI)

Figure 6. Erlotinib and selumetinib prevent PBMC-induced PD-L1, but not MHC-I expression in NSCLC cells. (A) H292 and H358 cells were cocultured with 72-hour pre-activated PBMCs from healthy volunteers at a ratio of 5 PBMCs per tumor cell. During coculture cells were treated with 20 ng/mL EGF, and 10 μM erlotinib or 10 μM selumetinib. After 24 hours, PD-L1 membrane expression (Two-way ANOVA with Bonferroni's multiple comparisons method ** P < 0.01, *** P < 0.01 compared to control + pre-activated PBMCs) (B) and MHC-I membrane expression were measured using flow cytometry (Two-way ANOVA * P < 0.05, ** P < 0.01 compared to control). (C) Proposed model for the role of IFNγ and MAPK signaling in PD-L1 regulation of lung adenocarcinoma. IFNγ derived from tumor infiltrating immune cells induces transcription of PD-L1 in tumor cells through activation of JAK/STAT-signaling. PD-L1 mRNA is translated into PD-L1 protein, which is transported to the cell membrane. Growth receptor- and KRAS mutation-induced MAPK signaling increases STAT signaling, potentially adding to transcriptional activity. Also, MAPK signaling increases stability of PD-L1 mRNA, resulting in increased mRNA and protein levels, and subsequently increasing PD-L1 membrane expression. R = resting PBMCs, A = activated PBMCs.